

# Modeling ecological drivers in marine viral communities using comparative metagenomics and network analyses

Bonnie L. Hurwitz<sup>a,1</sup>, Anton H. Westveld<sup>b,c</sup>, Jennifer R. Brum<sup>a</sup>, and Matthew B. Sullivan<sup>a,1</sup>

<sup>a</sup>Department of Ecology and Evolutionary Biology, University of Arizona, Tucson, AZ 85721; <sup>b</sup>Research School of Finance, Actuarial Studies and Applied Statistics, College of Business and Economics, Australian National University, Canberra, ACT 0200, Australia; and <sup>c</sup>Statistics Laboratory at the Bio5 Institute and Statistics Graduate Interdisciplinary Program, University of Arizona, Tucson, AZ 85721

Edited by David M. Karl, University of Hawaii, Honolulu, HI, and approved June 16, 2014 (received for review October 21, 2013)

Long-standing questions in marine viral ecology are centered on understanding how viral assemblages change along gradients in space and time. However, investigating these fundamental ecological questions has been challenging due to incomplete representation of naturally occurring viral diversity in single gene- or morphology-based studies and an inability to identify up to 90% of reads in viral metagenomes (viromes). Although protein clustering techniques provide a significant advance by helping organize this unknown metagenomic sequence space, they typically use only ~75% of the data and rely on assembly methods not yet tuned for naturally occurring sequence variation. Here, we introduce an annotation- and assembly-free strategy for comparative metagenomics that combines shared k-mer and social network analyses (regression modeling). This robust statistical framework enables visualization of complex sample networks and determination of ecological factors driving community structure. Application to 32 viromes from the Pacific Ocean Virome dataset identified clusters of samples broadly delineated by photic zone and revealed that geographic region, depth, and proximity to shore were significant predictors of community structure. Within subsets of this dataset, depth, season, and oxygen concentration were significant drivers of viral community structure at a single open ocean station, whereas variability along onshore-offshore transects was driven by oxygen concentration in an area with an oxygen minimum zone and not depth or proximity to shore, as might be expected. Together these results demonstrate that this highly scalable approach using complete metagenomic network-based comparisons can both test and generate hypotheses for ecological investigation of viral and microbial communities in nature.

virus | microbial ecology | Bayesian network

Microorganisms drive global biogeochemical cycles (1), with abundances and taxonomic composition tuned to spatio-temporally varying environmental conditions (2–5). Viruses then modulate these biogeochemical processes through mortality, horizontal gene transfer, and metabolic reprogramming (6). However, our understanding of how viral communities change in response to biological, physical, and chemical factors and host availability has been limited by technical challenges.

Most viruses in the ocean lack both cultivated representatives [85% of 1,100 sequenced phage genomes derive from only 3 of 45 bacterial phyla (7)] and a universally conserved marker gene (8); thus, metagenomics is commonly applied to characterize the ecology and evolution of viral assemblages. Problematically, however, our ability to investigate these assemblages via metagenomics remains limited by the lack of known viruses and viral proteins in biological sequence databases. The first viral metagenome (virome) used thousands of Sanger reads and found that 65% of sequences were unknown [i.e., no database match for reads >600 bp (9)]. Adoption of next-generation sequencing (NGS) technologies then generated hundreds of thousands of reads (averaging 102 bp in length) per virome and returned ~90% sequence novelty (10). This unknown problem has not

been significantly improved on in subsequent oceanic virome studies regardless of sequencing platform (11). This novelty limits taxonomic and functional inferences about viral assemblages and makes comparative analyses that only use the known portion of these datasets minimally informative at best and completely misleading at worst. Additionally, the standard practice of comparing new datasets against large genomic databases is compute intensive and increasingly unfeasible given escalating scales in datasets and databases.

To circumvent similar issues, Yooseph et al. (12) clustered environmental reads with known proteins from available databases to define sequence similarity-based protein clusters (PCs) to analyze the first global ocean microbial metagenomic datasets. This PC approach helps to both organize the vastly unknown sequence space in metagenomes and identify abundant proteins in environmental datasets even where taxonomy and function are unknown. Application of this approach to viromes has also been fruitful and has led to (i) a dataset of 456K protein clusters (11), (ii) comparative estimates of viral community diversity across sites (11, 13), and (iii) an estimate that the global virome is three orders of magnitude less diverse than previously thought (14). Although a valuable approach for metagenomic data, particularly for viromes where functional and taxonomic information is

## Significance

Microorganisms and their viruses are increasingly recognized as drivers of myriad ecosystem processes. However, our knowledge of their roles is limited by the inability of culture-dependent and culture-independent (e.g., metagenomics) methods to be fully implemented at scales relevant to the diversity found in nature. Here we combine advances in bioinformatics (shared k-mer analyses) and social networking (regression modeling) to develop an annotation- and assembly-free visualization and analytical strategy for comparative metagenomics that uses all the data in a unified statistical framework. Application to 32 Pacific Ocean viromes, the first large-scale quantitative viral metagenomic dataset, tested existing and generated further hypotheses about ecological drivers of viral community structure. Highly computationally scalable, this new approach enables diverse sequence-based large-scale comparative studies.

Author contributions: B.L.H. and A.H.W. designed research; B.L.H. and A.H.W. performed research; B.L.H. and A.H.W. contributed new reagents/analytic tools; B.L.H., A.H.W., and J.R.B. analyzed data; and B.L.H., A.H.W., J.R.B., and M.B.S. wrote the paper.

The authors declare no conflict of interest.

This article is a PNAS Direct Submission.

Freely available online through the PNAS open access option.

Data deposition: All methods and source code are fully documented and are freely available at <http://code.google.com/p/tmpl/>. Viromes are available in the iPlant Community Data folder (imicrobe/pov) at <http://www.iplantcollaborative.org/>.

<sup>1</sup>To whom correspondence may be addressed. Email: [bhurwitz@E-mail.arizona.edu](mailto:bhurwitz@E-mail.arizona.edu) or [mbsulli@E-mail.arizona.edu](mailto:mbsulli@E-mail.arizona.edu).

This article contains supporting information online at [www.pnas.org/lookup/suppl/doi:10.1073/pnas.1319778111/-DCSupplemental](http://www.pnas.org/lookup/suppl/doi:10.1073/pnas.1319778111/-DCSupplemental).



**Table 1. Bayesian inference numerical summaries for social networks with selected covariates**

| Network dataset/Covariate                  | Parameter | Posterior median | Lower limit credible interval (2.5%) | Upper limit credible interval (97.5%) |
|--|-----------|------------------|--------------------------------------|---------------------------------------|
| Full dataset [32 samples (nodes)]          |           |                  |                                      |                                       |
| $\log(\bar{n}_{i,j})$                      | $\gamma$  | 0.63             | <b>0.42</b>                          | <b>0.88</b>                           |
| <b>Geographic region</b>                   | $\beta_1$ | 0.14             | <b>0.06</b>                          | <b>0.21</b>                           |
| <b>Depth</b>                               | $\beta_2$ | 0.12             | <b>0.06</b>                          | <b>0.19</b>                           |
| Season                                     | $\beta_3$ | 0.03             | -0.02                                | 0.08                                  |
| <b>Proximity to shore</b>                  | $\beta_4$ | 0.12             | <b>0.08</b>                          | <b>0.16</b>                           |
| Oxygen                                     | $\beta_5$ | -0.00            | -0.21                                | 0.08                                  |
| LineP open ocean [11 samples (nodes)]      |           |                  |                                      |                                       |
| $\log(\bar{n}_{i,j})$                      | $\gamma$  | 0.828            | <b>0.206</b>                         | <b>1.298</b>                          |
| <b>Depth</b>                               | $\beta_1$ | 0.224            | <b>0.11</b>                          | <b>0.343</b>                          |
| <b>Season</b>                              | $\beta_2$ | 0.124            | <b>0.032</b>                         | <b>0.257</b>                          |
| <b>Oxygen</b>                              | $\beta_3$ | -0.336           | <b>-0.589</b>                        | <b>-0.084</b>                         |
| LineP spring transect [11 samples (nodes)] |           |                  |                                      |                                       |
| $\log(\bar{n}_{i,j})$                      | $\gamma$  | 6.737            | <b>5.555</b>                         | <b>7.874</b>                          |
| Depth                                      | $\beta_1$ | 0.117            | -0.053                               | 0.287                                 |
| Proximity to shore                         | $\beta_2$ | 0.047            | -0.063                               | 0.147                                 |
| <b>Oxygen</b>                              | $\beta_3$ | 0.867            | <b>0.253</b>                         | <b>1.205</b>                          |

Statistically significant covariates for each network are shown in bold. Covariates are considered significant if the upper and lower credible intervals (Bayesian confidence intervals) do not overlap with zero. The covariate  $\log(\bar{n}_{ij})$  is an offset (although we do not restrict the coefficient to be equal to 1), which accounts for the fact that more shared read space may occur between two viromes if the either of the viromes is larger.

P26 station. Visually, again upper ocean, photic zone viromes were clearly separated from deep water, aphotic zone viromes, with seasonality leading to structure within these zones (Fig. 1C). Statistical regressions suggested that ecological drivers included depth, season, and oxygen concentration (Table 1).

A second subset of the data from LineP allowed focus on spatial variability from the coastal to open ocean samples collected on a springtime research cruise (Fig. 1D). Visually, again the photic and aphotic zone viromes were separated in shared k-mer space, but this time no strong patterns were observed with depth within these larger zones or with proximity to shore. Statistical analyses supported these qualitative observations, as only oxygen represented a structuring factor (Table 1).

**LineP: A Case Study in Niche Specialization by Season.** The power of the above analyses is the ability to visually represent viromes and define significant metadata factors to drive further investigation into underlying patterns. Given that reads have associated abundances (via the k-mer mode; *SI Methods* and [Figs. S2 and S3](#)), reads that are exclusive to specific viromes or parts of the network can be mined out of the underlying data. We demonstrate this by examining reads that are distinct by season (summer vs. winter) and photic zone (photic vs. aphotic) at open ocean station P26 at LineP in the Pacific Ocean based on [Fig. 1C](#) and [Table 1](#). The exclusive read data demonstrate metabolic differences in parts of the network that likely derive from viral-encoded auxiliary metabolic genes as follows ([Fig. 2](#)), given the purity of these viromes (11, 13, 26).

The largest proportion of exclusive reads in all viromes, irrespective of photic zone or season, encodes genes related to nucleotide metabolism (Fig. 2). Given that viruses require nucleotides for replication, this result is not unexpected. When broadly comparing the photic zone and aphotic zone, aphotic viromes contain more overall metabolic functional capacity. In particular, genes related to the tricarboxylic acid (TCA) cycle, mannose and fructose metabolism, and electron transport chain (ETC) are more highly represented in aphotic viromes and are likely involved in energy production (26). These genes may be less represented in photic samples, given the capacity for viruses to encode and express photosynthetic genes (6) that allow them to derive energy for phage replication. Fatty acid metabolism may also be a source of energy production in phage in all seasons and photic zones, but most highly represented in summer aphotic viromes perhaps due to increased

phage production in the summer and less energy derived from other sources. Interestingly, aphotic viromes and winter photic viromes contain genes related to cysteine and methionine metabolism, whose role is currently unknown but may be related to scavenging iron from Fe-S clusters in iron limited regions given that cysteine is important for Fe-S cluster biogenesis and degradation (27). Last, pyrimidine, purine, and glutathione metabolism may be important in winter aphotic viromes. Given that glutathione improves cold resistance in bacteria (28), viruses may help to provide protection to their infected hosts in the winter. These data suggest that viruses coevolve with their hosts and bolster host metabolism to improve host vitality for phage production given environmental selective pressures on the host.

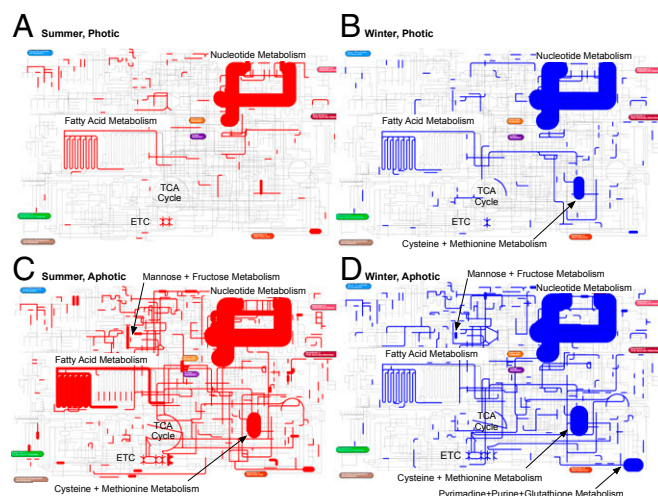


**Fig. 2.** Map of viral-encoded metabolic host genes from summer/winter and photic/aphotic at open ocean station P26 at LineP in the Pacific Ocean. The width of the lines corresponds to the normalized read abundance for viral encoded host genes in metabolic pathways from (A) summer photic (10 m) virome at LineP P26, (B) winter photic (10 m) virome at LineP P26, (C) summer aphotic (500, 1,000, and 2,000 m) viromes at LineP P26, and (D) winter aphotic (500, 1,000, and 2,000 m) viromes at LineP P26. ETC, electron transport chain. For map generation, see ref. S9.





effects and as a result allows for the proper inference for regression coefficients (i.e., metadata). Or, in simple terms, the distances between viromes based on shared reads can be visually represented, while at the same time accounting for biological factors in a single statistical model. The importance of single modeling and inferential framework is highlighted in Chiu and Westveld (25).

This approach is also inherently different from other statistical frameworks [e.g., MaAsLin (49)] that identify associations between metadata and the abundance of operational taxonomic units (OTUs) or functions in metagenomic samples. Specifically, MaAsLin outputs a list of OTUs or functions that are significant given a metadata type. Given that the results are granular (by OTU or function) and only account for only one metadata type at a time, they cannot be combined. In contrast, our analytical framework (i) uses a model that enables simultaneous examination of shared sequence space between viromes in conjunction with multiple metadata types and (ii) requires no prior organizational bins (e.g., OTUs for MaAsLin), which is critical for viruses that lack a universal barcode gene for such taxonomic assignments. Both advances are fundamental for surveying complex viral communities to look for ecological drivers of community structure but also help broaden the toolkit available for other comparative metagenomic datasets (e.g., bacterial).

This approach may also prove to be important in other microbial analyses wherein taxonomic identification is less of a concern given rRNA sequence datasets. Specifically, we use entire metagenomes rather than a single gene (like 16S in bacteria) to assess the composition of microbial communities. The use of complete metagenomes is particularly important in cases where metagenomes may contain closely related species, indistinguishable on the level of the 16S gene alone, that have functional differences that make them distinct.

Further, because reads that represent significant patterns in the network can be mined out (see results LineP seasonal niche differentiation), this approach drives functional comparative metagenomic analyses. This approach is also important pragmatically in terms of runtime because fewer reads require extensive functional annotation. Moreover, the remaining unknown fraction of reads exclusive to a certain part of the network provides a starting point for future empirical analyses to understand the function of novel viral species. This approach is broadly applicable to metagenomes comprised of any microbe from viruses, to bacteria or fungi, and extends current approaches through the use of whole metagenomes and a comprehensive statistical framework.

**Conclusions.** Although marine microbes and their viruses are fundamental to Earth system function, the culture-independent metagenomic techniques used to study them present “big data” analytical challenges. The combination of shared k-mer and social network analysis presented here provides a powerful way to visualize and explore relationships between metagenomic samples and populations and statically evaluate the underlying factors that drive this variability. These methods are computationally tractable and widely applicable across sequence datasets and have the capacity to affect how data are stored, visualized, and analyzed, making use of big data analytics and the large-scale context that is now becoming available in metagenomic data repositories. These types of analyses and scales of data are needed to predictively model Earth’s most abundant biological entities, viruses, and their predominant hosts, microorganisms.

## Methods

Methods detailed below are further documented in *SI Methods*, Figs. S2 and S3, and Tables S1–S4. All source code is freely available at ref. 50.

**Dataset.** The 32-virome POV dataset (Table S3) (11) was examined to identify patterns of sequence similarity in viromes and determine the relationship between these patterns and depth, season, proximity to shore, geographic distance, and oxygen concentration. This dataset is a recently available

public resource that leverages well-characterized sample-to-sequence preparation methods to generate quantitative viromes (13, 31). A full description of metadata associated with each virome and methods used to prepare the viromes and perform read quality control is included in *SI Methods* and Table S3. One additional filtering step was applied beyond the quality control steps for the POV dataset (11) that entailed removing reads with low abundance k-mers (k-mer = 1) in their own virome that were suspected of being contaminants (13) and reads with high-abundance k-mers (>1,000) that are likely to be either sequencing artifacts or highly conserved protein domains that may distort the overall abundance of that read.

**k-mer Analyses.** In the k-mer analysis below, suffix arrays were created using mkvtree from the vmatch package version 2.1.5 (51) using parameters (-pl -allout -v). Reads were compared with suffix arrays using vmatch’s vmerstat (-minocc 1 -counts) to search for the frequency of 20-bp k-mers across the read. The k-mer size was set by examining the uniqueness ratio in the dataset (52). The k-mer value of 20 was chosen given that it represented an inflection point where k-mer hits moved from random to representative of the sequence content.

**Pairwise All-vs.-All Analysis of Viromes.** High-quality reads for each virome were compared with suffix arrays from all other viromes in a pairwise fashion (compute pipeline kmercompare.tar) to achieve an all-vs.-all analysis of the viromes [virome  $i$  vs. virome  $j$ , (for  $i = 1, \dots, 32$ ) and (for  $j = 1, \dots, 32$ )]. The abundance for each read (in virome  $i$ ) was calculated by finding the mode k-mer value for all k-mers in that read compared with the virome  $j$  suffix array (*SI Methods* and Figs. S2 and S3). This analysis resulted in a single abundance value (k-mer mode) for each read in virome  $i$  compared with virome  $j$ . The data were then normalized by averaging ( $\bar{y}_{i,j}$ ) (shared read count) and ( $\bar{n}_{i,j}$ ) (total read count) between virome  $i$  and virome  $j$ . Normalized shared read counts were used to construct a  $32 \times 32$  matrix of viromes.

**Network Analysis.** To model the valued (nonbinary) nondirected data above, we consider the latent space approach outlined in Eq. 1 (23–25, 53). Our network modeling framework, via random effects, decomposes the statistical variation in the data to account for (i) the activity level ( $a_i$ ) of each virome  $i$  (average amount of sequence space shared across the network for each virome  $i$ ) and (ii) similarity (clustering) of shared sequence amount among viromes. For  $i$ ,  $z_i^T z_j$  is measure of distance and similarity between viromes  $i$  and  $j$ . Each virome’s position ( $z_i$ ) may be visualized in a  $k$ -dimensional latent space  $Z$  (after a Procrustes’ transformation to convert into a similar grid to compare) where virome  $i$  and virome  $j$  are considered similar if they are close in that space. For ease of visualization, we consider the case where  $k=2$  (ref. 53 considered a 1D space).

Finally, we account for a set of relational covariates ( $x_{ij} = 1$  if similar, 0 if not) based on geographic region, season, proximity to shore, depth, and oxygen concentration using values in Table S3. In the case of oxygen concentration, which is a continuous value, high and low oxygen values were determined based on a cutoff of 0.06 mL/L.

$$\begin{aligned} \log(\bar{y}_{i,j}) &= \alpha + \gamma \log(\bar{n}_{i,j}) + \beta' x_{ij} + a_i + a_j + z_i^T z_j + \varepsilon_{ij} \\ i &< j, \\ a_i &\sim \text{identically distributed normal}(0, \sigma_a^2), \\ z_{i,1} &\sim \text{identically distributed normal}(0, \sigma_{z1}^2), \\ z_{i,2} &\sim \text{identically distributed normal}(0, \sigma_{z2}^2), \\ \varepsilon_{ij} &\sim \text{identically distributed normal}(0, \sigma_\varepsilon^2). \end{aligned} \quad [1]$$

To estimate the parameters in the model, a Bayesian inferential approach was considered using the R statistical software (54) and gbme.R obtained from refs. 24 and 55. For our analyses, empirical Bayes priors were considered (the default for the gbme.R). To examine the joint posterior distribution of the parameters, a Markov chain of 1,000,000 scans was constructed. The first 500,000 scans were removed for burn-in, and the chain was thinned by every 100th scan, leaving 5,000 samples.

**Construction of Euler Diagrams Depicting Shared Read Content in Networks.** Using data from the pairwise k-mer analysis described above, reads were detected that were unique or shared between subsets of viromes that visually clustered in the networks using a PERL script (get\_section.pl). Reads were considered exclusive if they were present (mode k-mer  $\geq 2$ ) in two or more viromes in a cluster and absent (mode k-mer  $< 2$ ) from viromes outside that cluster. For single virome clusters, all reads that were not shared with other viromes and present within that single virome at a k-mer abundance  $> 2$  were considered exclusive. Reads that were present in a virome just once

(k-mer = 1) were removed from the analysis given a higher probability of contamination (13) per the discussion above. The results were then used to compute an Euler diagram using the *venneuler* function (56) in the R statistical software (54).

**Annotating Exclusive Reads.** Exclusive reads per the method above for LineP summer photic viromes, summer aphotic viromes, winter photic viromes, and winter aphotic viromes were compared against the similarity matrix of proteins (SIMAP) released on August 20, 2013 (57) using BLASTX (58) to assign function as previously described (22). Briefly, these analyses were implemented using a custom data analysis pipeline written in Perl and bash shell and executed on a high-performance computer using PBSPro (blastpipeline\_simap.tar). Hits were considered significant if they had an E value < 0.001, and only top hits were retained. Interpro ids in the SIMAP functional annotation were mapped to EC numbers using the *swissprot\_kegg\_proteins\_ec.csv* as a mapping (59) (*ipr\_to\_ec.pl*). Read hit counts were normalized based on

sequencing effort in the included viromes and converted into ipath2 format (*create\_ipath.pl*) for visual representation in the ipath2 viewer (58).

**ACKNOWLEDGMENTS.** We thank Tucson Marine Phage Laboratory members for comments on the manuscript; D. D. Billheimer for statistics support; E. Allers, L. Deng, M. Dude-Duhaime, B. Poulos, J. Wright, K. Mitchell, C. Mewis, and A. Worden for logistical support, sample collection, and/or processing of viral concentrates; and University Information Technology Services Research Computing Group for high throughput computing access and support. Sequencing was provided by the US Department of Energy Joint Genome Institute Community Sequencing Program under the Office of Science of the US Department of Energy Contract DE-AC02-05CH11231 and the Gordon and Betty Moore Foundation Marine Microbial Initiative, whereas funding was from National Science Foundation Grants DBI-0850105 and OCE-0961947, Biosphere 2, BIO5, and Gordon and Betty Moore Foundation Grant GBMF3790 (to M.B.S.), as well as an Integrative Graduate Education Research Traineeship and National Science Foundation graduate research fellowship (to B.L.H.).

- Falkowski PG, Fenchel T, DeLong EF (2008) The microbial engines that drive Earth's biogeochemical cycles. *Science* 320(5879):1034–1039.
- Caporaso JG, Paszkiewicz K, Field D, Knight R, Gilbert JA (2012) The Western English Channel contains a persistent microbial seed bank. *ISME J* 6(6):1089–1093.
- Chow CE, Fuhrman JA (2012) Seasonality and monthly dynamics of marine myovirus communities. *Environ Microbiol* 14(8):2171–2183.
- Fortunato CS, Herfort L, Zuber P, Baptista AM, Crump BC (2012) Spatial variability overwhelms seasonal patterns in bacterioplankton communities across a river to ocean gradient. *ISME J* 6(3):554–563.
- Zaikova E, et al. (2010) Microbial community dynamics in a seasonally anoxic fjord: Saanich Inlet, British Columbia. *Environ Microbiol* 12(1):172–191.
- Breitbart M (2012) Marine viruses: Truth or dare. *Annu Rev Mar Sci* 4:425–448.
- Holmfeldt K, et al. (2013) Twelve previously unknown phage genera are ubiquitous in global oceans. *Proc Natl Acad Sci USA* 110(31):12798–12803.
- Edwards RA, Rohwer F (2005) Viral metagenomics. *Nat Rev Microbiol* 3(6):504–510.
- Breitbart M, et al. (2002) Genomic analysis of uncultured marine viral communities. *Proc Natl Acad Sci USA* 99(22):14250–14255.
- Angly FE, et al. (2006) The marine viromes of four oceanic regions. *PLoS Biol* 4(11):e368.
- Hurwitz BL, Sullivan MB (2013) The Pacific Ocean virome (POV): A marine viral metagenomic dataset and associated protein clusters for quantitative viral ecology. *PLoS ONE* 8(2):e57355.
- Yooseph S, et al. (2007) The Sorcerer II Global Ocean Sampling expedition: Expanding the universe of protein families. *PLoS Biol* 5(3):e16.
- Hurwitz BL, Deng L, Poulos BT, Sullivan MB (2013) Evaluation of methods to concentrate and purify ocean virus communities through comparative, replicated metagenomics. *Environ Microbiol* 15(5):1428–1440.
- Ignacio-Espinoza JC, Solonenko SA, Sullivan MB (2013) The global virome: Not as big as we thought? *Curr Opin Virol* 3(5):566–571.
- Degnan PH, Ochman H (2012) Illumina-based analysis of microbial community diversity. *ISME J* 6(1):183–194.
- Edwards RA, et al. (2012) Real time metagenomics: Using k-mers to annotate metagenomes. *Bioinformatics* 28(24):3316–3317.
- Song K, et al. (2013) Alignment-free sequence comparison based on next-generation sequencing reads. *J Comput Biol* 20(2):64–79.
- Jiang B, et al. (2012) Comparison of metagenomic samples using sequence signatures. *BMC Genomics* 13:730.
- Dinsdale EA, et al. (2008) Functional metagenomic profiling of nine biomes. *Nature* 452(7187):629–632.
- Williamson SJ, et al. (2008) The Sorcerer II Global Ocean Sampling Expedition: Metagenomic characterization of viruses within aquatic microbial samples. *PLoS ONE* 3(1):e1456.
- Bench SR, et al. (2007) Metagenomic characterization of Chesapeake Bay viroplankton. *Appl Environ Microbiol* 73(23):7629–7641.
- Hoff PD, Raftery A, Handcock M (2002) Latent space approaches to social network analysis. *J Am Stat Assoc* 97(460):1090–1098.
- Hoff PD (2005) Bilinear mixed-effects models for dyadic data. *J Am Stat Assoc* 100(469):286–295.
- Chiu GS, Westveld AH (2011) A unifying approach for food webs, phylogeny, social networks, and statistics. *Proc Natl Acad Sci USA* 108(38):15881–15886.
- Hurwitz BL, Hallam SJ, Sullivan MB (2013) Metabolic reprogramming by viruses in the sunlit and dark ocean. *Genome Biol* 14(11):R123.
- Sharon I, et al. (2011) Comparative metagenomics of microbial traits within oceanic viral communities. *ISME J* 5(7):1178–1190.
- Zhang J, Li Y, Chen W, Du GC, Chen J (2012) Glutathione improves the cold resistance of *Lactobacillus sanfranciscensis* by physiological regulation. *Food Microbiol* 31(2):285–292.
- Breitbart M, Rohwer F (2005) Here a virus, there a virus, everywhere the same virus? *Trends Microbiol* 13(6):278–284.
- Brum JR, Schenck RO, Sullivan MB (2013) Global morphological analysis of marine viruses shows minimal regional variation and dominance of non-tailed viruses. *ISME J* 7(9):1738–1751.
- Duhaime MB, Sullivan MB (2012) Ocean viruses: Rigorously evaluating the metagenomic sample-to-sequence pipeline. *Virology* 434(2):181–186.
- Ladau J, et al. (2013) Global marine bacterial diversity peaks at high latitudes in winter. *ISME J* 7(9):1669–1677.
- Brown MV, et al. (2012) Global biogeography of SAR11 marine bacteria. *Mol Syst Biol* 8:595.
- Coleman ML, Chisholm SW (2007) Code and context: *Prochlorococcus* as a model for cross-scale biology. *Trends Microbiol* 15(9):398–407.
- Weinbauer MG (2004) Ecology of prokaryotic viruses. *FEMS Microbiol Rev* 28(2):127–181.
- DeLong EF, et al. (2006) Community genomics among stratified microbial assemblages in the ocean's interior. *Science* 311(5760):496–503.
- Jiang S, Fu W, Chu W, Fuhrman JA (2003) The vertical distribution and diversity of marine bacteriophage at a station off Southern California. *Microb Ecol* 45(4):399–410.
- Steward G, Montiel JL, Azam F (2000) Genome size distributions indicate variability and similarities among marine viral assemblages from diverse environments. *Limnol Oceanogr* 45(8):1697–1706.
- Freeland H (2007) A short history of ocean station papa and Line P. *Prog Oceanogr* 75(2):120–125.
- Whitney FA, Freeland HJ, Robert M (2007) Persistently declining oxygen levels in the interior waters of the eastern subarctic Pacific. *Prog Oceanogr* 75(2):179–199.
- Parsons RJ, Breitbart M, Lomas MW, Carlson CA (2012) Ocean time-series reveals recurring seasonal patterns of viroplankton dynamics in the northwestern Sargasso Sea. *ISME J* 6(2):273–284.
- Gilbert JA, et al. (2012) Defining seasonal marine microbial community dynamics. *ISME J* 6(2):298–308.
- Wright JJ, Konwar KM, Hallam SJ (2012) Microbial ecology of expanding oxygen minimum zones. *Nat Rev Microbiol* 10(6):381–394.
- Brum JR, Steward GF (2010) Morphological characterization of viruses in the stratified water column of alkaline, hypersaline Mono Lake. *Microb Ecol* 60(3):636–643.
- Cassman N, et al. (2012) Oxygen minimum zones harbour novel viral communities with low diversity. *Environ Microbiol* 14(11):3043–3065.
- Whitney F, Crawford WR, Harrison PJ (2005) Physical processes that enhance nutrient transport and primary productivity in the coastal and open ocean of the subarctic NE Pacific. *Deep Sea Res Part II Top Stud Oceanogr* 52(5):681–706.
- Allers E, et al. (2013) Diversity and population structure of Marine Group A bacteria in the Northeast subarctic Pacific Ocean. *ISME J* 7(2):256–268.
- Dinsdale EA, et al. (2013) Multivariate analysis of functional metagenomes. *Front Genet* 4:41.
- Huttenhower C (2014) MaAsLin: Multivariate analysis by linear models. Available at <http://huttenhower.sph.harvard.edu/maaslin>. Accessed December 30, 2013.
- Hurwitz BL (2014) Tmpl source code. Available at <http://code.google.com/p/tmpl>. Accessed December 30, 2013.
- vmatch (2013) vmatch package version 2.1.5. Available at [www.vmatch.de](http://www.vmatch.de).
- Kurtz S, Narechania A, Stein JC, Ware D (2008) A new method to compute K-mer frequencies and its application to annotate large repetitive plant genomes. *BMC Genomics* 9:517.
- Chiu GS, Westveld AH (2014) A statistical social network model for consumption data in trophic food webs. *Stat Methodol* 17(4432):139–160.
- R Core Team (2012) *R: A Language and Environment for Statistical Computing* (R Foundation for Statistical Computing, Vienna).
- Hoff P (2013) gbme.R. [http://www.stat.washington.edu/hoff/Code/hoff\\_2005\\_jasa](http://www.stat.washington.edu/hoff/Code/hoff_2005_jasa). Accessed on December 31, 2013.
- Wilkinson L (2012) Exact and approximate area-proportional circular Venn and Euler diagrams. *IEEE Trans Vis Comput Graph* 18(2):321–331.
- Rattei T, et al. (2006) SIMAP: the similarity matrix of proteins. *Nucleic Acids Res* 34(Database issue):D252–D256.
- Yamada T, Letunic I, Okuda S, Kanehisa M, Bork P (2011) iPath2.0: Interactive pathway explorer. *Nucleic Acids Res* 39(Web Server issue):W412–W415.
- De Ferrari L, Aitken S, van Hemert J, Goryanin I (2012) EnzML: Multi-label prediction of enzyme classes using InterPro signatures. *BMC Bioinformatics* 13:61.
- Altschul SF, et al. (1997) Gapped BLAST and PSI-BLAST: A new generation of protein database search programs. *Nucleic Acids Res* 25(17):3389–3402.